Phase behavior and structure of aqueous dispersions of sphingomyelin

G. Graham Shipley, Leonard S. Avecilla, and Donald M. Small

Biophysics Division, Department of Medicine, Boston University School of Medicine, Boston, Massachusetts 02118

Abstract The phase behavior of bovine brain sphingomyelin in water has been determined by polarizing light microscopy, differential scanning calorimetry, and X-ray diffraction. Lamellar phases, in which water is intercalated between sheets of lipid molecules arranged in the classical bilayer fashion, are present over much of the phase diagram. An order–disorder transition separates the high temperature, liquid crystalline, lamellar phase from a more ordered lamellar phase at low temperatures. The hydration characteristics of sphingomyelin are similar to the structurally related lecithin in that only limited amounts of water are incorporated above and below the transition. Above the transition at 47°C, a maximum of 35% by weight of water can be incorporated between the lipid bilayers, the total thickness at maximum hydration being 60.2 Å, the lipid thickness 38 Å, and the surface area per lipid molecule at the interface 60 Å^2. Water in excess of 35% by weight is present as a separate phase.

Below the phase transition, at 25°C a maximum of 42% by weight of water may be incorporated between the lipid bilayers. On increasing the hydration, the lamellar repeat distance increases from 63.5 Å to a limiting value of 76 Å. Within this hydration range the calculated lipid thickness decreases from 63.5 to 42.5 Å, and the surface area per lipid molecule increases from 36.1 to 53.6 Å^2. Although these changes may be accounted for by a structure in which the hexagonally packed ordered hydrocarbon chains tilt progressively with respect to the normal to the bilayer plane on increasing hydration, it is possible that changes in other more complex lamellar structures may be responsible for these variations in lipid thickness and surface area.

Supplementary key words phospholipids · cell membranes · atherosclerosis · X-ray diffraction · differential scanning calorimetry · polarizing light microscopy · lamellar liquid crystals · order–disorder phenomena

The occurrence of large amounts of sphingomyelin in the membranes of brain and nerve tissues and its variable presence in erythrocyte membranes from different animal species have been well documented (1). Of particular interest is the observation by de Gier and van Deenen (2) that for several animal species the phosphatidylcholine (lecithin) content of erythrocyte membranes decreases as the sphingomyelin content increases. Furthermore, chemical binding studies on intact erythrocytes are consistent with the concept of an asymmetric distribution of lipids in erythrocyte membranes, the two choline-containing lipids being located primarily on the outside of the membrane (3, 4). Sphingomyelin occurs in the four major classes (high density, low density, very low density, and chylomicrons) of serum lipoproteins (5), and perhaps of fundamental importance in terms of aging and arterial disease is the involvement of sphingomyelin and other lipids in the accumulation of lipids in arterial tissues (6, 7). Again, there appears to be some metabolic relationship between sphingomyelin and other phospholipids in that as the relative amount of the former increases in arterial tissue with age, so lecithin, in particular, declines (8).

Although the physical properties and behavior of many important phospholipid classes have been well defined by a variety of physicochemical methods (for example, see Refs. 9–11), the paucity of information on sphingomyelin permits only limited comparisons with these other lipid classes. The surface properties of beef heart sphingomyelin and dipalmitoyl phosphatidylcholine were compared by Shah and Schulman (12, 13), and although the limiting surface areas occupied by the two lipids were identical (~ 44 Å^2), their surface potential behavior differed markedly. The phase behavior of sphingomyelin in water was reported by Reiss-Husson (14), who showed that at 40°C sphingomyelin formed a bimolecular, lamellar phase with the limited hydration or swelling property similar to that exhibited by various phosphatidylcholines. More recently, limited studies of the interaction of cholesterol with sphingomyelin have been reported, utilizing the techniques of differential scanning calorimetry and nuclear magnetic resonance (15) and electron spin resonance spectroscopy (16), and it appears that cholesterol influences or modifies

Abbreviations: DSC, differential scanning calorimetry. 1 Å ≡ 10^{-1} nm.

the hydrocarbon chain packing and chain melting behavior of sphingomyelin.

As part of a program aimed at investigating the mutual interaction of lipids important in membranes and lipoproteins, we report here a detailed study of the phase behavior of aqueous dispersions of sphingomyelin, utilizing polarized light microscopy, differential scanning calorimetry, and X-ray diffraction. A subsequent paper will discuss the effect of cholesterol on this phase behavior.

MATERIALS

Bovine brain sphingomyelin (grade 1; Lipid Products, Epsom, England) was shown to be pure (>99%) by thin-layer chromatography. Sphingomyelin was refluxed for 1 hr at 100°C with 10% boron trifluoride in methanol, and analysis of the fatty acid methyl esters was performed on a Hewlett-Packard model 700 gas–liquid chromatograph equipped with a dual flame ionization detector. Separation was achieved with a 6-ft × ⅛ inch OD stainless steel column packed with 20% diethylene glycol succinate polyester on 90–100 mesh Anakrom A. The column and detector ovens were maintained at 200°C and 240°C, respectively. The composition of the fatty acid linked through the amide group to the sphingosine base is shown in Table 1. The molecular weight computed on the basis of the fatty acid composition was 767. The water used was doubly distilled, the last distillation being over potassium permanganate.

METHODS

Sample preparation

Acid-washed Pyrex tubes with a narrow constriction at the center were used for the solvent evaporation, hydration, and equilibration procedures. After injection of the lipid, dissolved in chloroform–methanol 2:1 (v/v), the tube was purged with nitrogen and the solvent was removed in a vacuum desiccator over phosphorus pentoxide at 25°C. After addition of the appropriate amount of water needed to produce the desired concentration, the tube was once again purged with nitrogen and promptly sealed.

Equilibration of mixtures with a lipid concentration (c = g of lipid/[g of lipid + g of water]) in the range $0.7 > c > 0.4$ was achieved by repeated centrifugation, at 47°C, of the sample back and forth through the sample tube constriction for periods of 4–8 hr. For dispersions with $1.0 > c > 0.7$, the temperature of centrifugation was maintained about 10°C higher than the projected liquid crystal transition temperature. At the end of the equilibration procedure, the tube was opened and samples were taken immediately for gravimetric analysis of water content, light microscopy, thermal analysis, and X-ray diffraction.

Microscopy

A small quantity of the dry or hydrated sphingomyelin specimen was placed on a glass slide and covered immediately with a cover slip. The sample was observed under direct and polarized light on a Zeiss Standard NL microscope fitted with a heating stage. The number of phases present and their optical textures were observed as the temperature was raised at ~2°C/min. Gross rheological changes in the sample were identified by observation of the ease with which the cover slip could be displaced. Dry sphingomyelin was studied in the temperature range 25–250°C and hydrated mixtures from 25 to 100°C.

Differential scanning calorimetry

Small samples (5–10 mg) were hermetically sealed in aluminum pans, and a variety of heating and cooling runs in the temperature range −60 to 100°C were recorded, using a DuPont 900 differential thermal analyzer with a scanning calorimeter attachment.

X-ray diffraction

Samples were sealed either in thin-walled glass capillaries or between the Mylar or mica windows of a variable-temperature sample holder. X-ray diffraction patterns were recorded on an Elliott toroidal camera (17) adapted to the high intensity, 200-μm spot, X-ray beam from an Elliott GX6 rotating anode generator. Using CuK_α radiation, diffraction patterns in the range 3–80 Å were recorded at different temperatures with exposure times of approximately 1 hr. Occasionally, diffraction patterns were obtained using the slit-collimation system of a Luzzati-Baro camera. The methods used to calculate the lipid thickness (d_l) and surface area per molecule (S) from primary diffraction data (d), lipid concentration (c), molecular weight, and ratio of partial specific volumes of the two components ($\bar{v}_w/\bar{v}_l$) have been described in detail by Luzzati (10). For all calculations the molecular weight used was 767 (see above), and the ratio of the partial specific volumes was assumed to be 1.11.

RESULTS

The amide-linked fatty acid composition of bovine brain sphingomyelin shown in Table 1 is dominated by two fatty acid species, $C_{18:0}$ and $C_{24:1}$. It seems probable that the combination of the sphingosine chain with this relatively simple fatty acid distribution may account, at least in part, for the melting behavior described below (see Figs. 1 and 2).

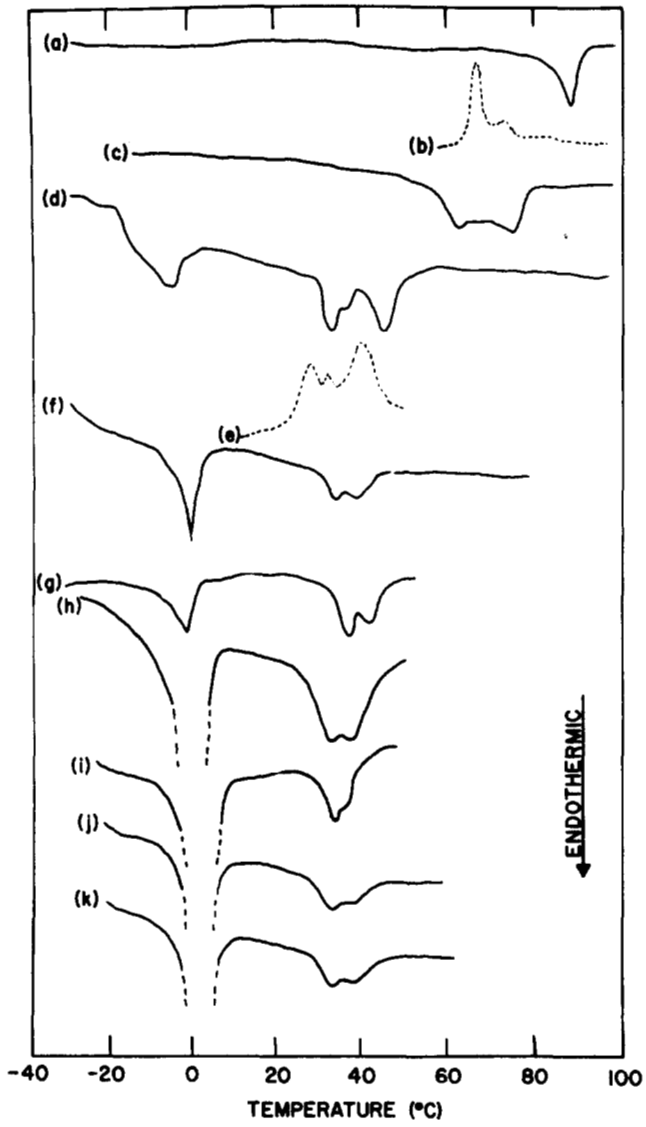

Fig. 1. Representative differential scanning calorimetry heating (——) and cooling (···) curves of sphingomyelin–water mixtures (heating/cooling rates 5°C/min). (*a*) and (*b*), c = 1.0; (*c*) = 0.939; (*d*) and (*e*), c = 0.855; (*f*), c = 0.786; (*g*), c = 0.729; (*h*), c = 0.650; (*i*), c = 0.580; (*j*), c = 0.523; (*k*), c = 0.455.

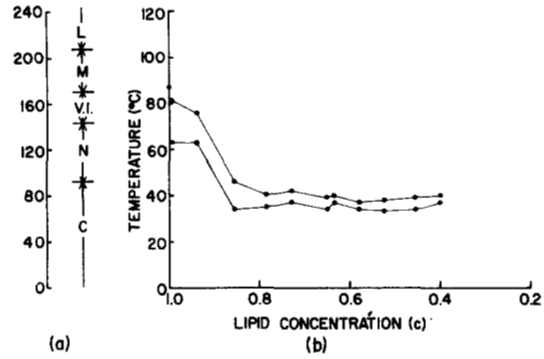

Fig. 2. (*a*) Optical textures exhibited by anhydrous sphingomyelin as a function of temperature. C represents crystal; N, neat; V.I., viscous isotropic; M, middle; and L, isotropic liquid. (*b*) Plot of differential scanning calorimetry transitions (heating) as a function of lipid concentration.

Microscopy

The gross features of the phase diagram were recognized from textural and rheological changes occurring in each sphingomyelin–water sample as the temperature was raised. In the dry state, sphingomyelin was present as very small, highly birefringent, rigid crystals. On raising the temperature, no obvious changes were observed until it reached 87°C, when a crystal to liquid crystal transition was observed. The anisotropic liquid crystal phase exhibited a neat phase texture (18, 19) and was stable over the temperature range 87–144°C. At 144°C, a viscous, optically isotropic phase formed that persisted until 170°C, whereupon another birefringent phase developed. This phase exhibited the classical middle phase texture (18, 19), notably at higher temperatures, before undergoing the transition to the optically isotropic fluid melt at 208°C. This behavior is summarized in Fig 2*a*.

The addition of small amounts of water produced a homogeneous birefringent phase with fairly viscous flow properties at low temperatures. On heating, this phase transformed over a fairly wide temperature range (~10°C) into a more fluid phase with the texture associated with the neat or lamellar lipid–water phase. The temperature limits of this transition decreased on increasing the amount of water present until a limit, 30–40°C, was reached at a hydration level equivalent to a lipid concentration of ≃0.85. For mixtures with c < 0.6, water could in some cases be observed as a separate phase. At high water contents, when water becomes the continuous phase, the maximally hydrated lamellar phase exists as optically positive anisotropic droplets.

Differential scanning calorimetry

The results obtained by differential scanning calorimetry (DSC) are summarized in Figs. 1 and 2. Fig. 1 shows DSC thermograms of sphingomyelin at different hydration levels. In the absence of water (Fig. 1, *a*), a single endothermic peak with the peak maximum at 87°C is observed on heating. Cooling anhydrous sphingomyelin resulted not only in supercooling but also in the separation into two distinct peaks (see Fig. 1, *b*) with peak maxima at 65 and 74°C. The addition of small amounts of water results in

TABLE 1. Fatty acid composition of bovine brain sphingomyelin

Fatty Acid	% (by wt)	Fatty Acid	% (by wt)
16:0[a]	3.9	22:0	6.2
17:0	0.6	20:4	1.3
18:0	44.8	23:0	2.1
19:0	0.5	23:1	1.4
20:0	2.8	24:0	5.1
21:0	0.4	24:1	27.4
		25:1	3.2

[a] Number of carbon atoms:number of double bonds.

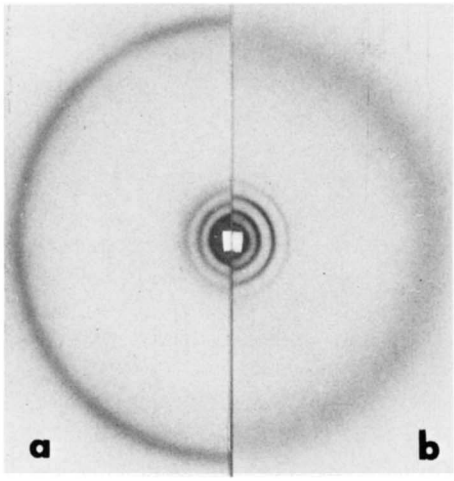

Fig. 3. X-ray diffraction patterns of sphingomyelin–water (c = 0.6) at (*a*) 25°C, showing the sharp diffraction line at 4.15 Å, and (*b*) 47°C, showing the broad, diffuse diffraction line at 4.6 Å.

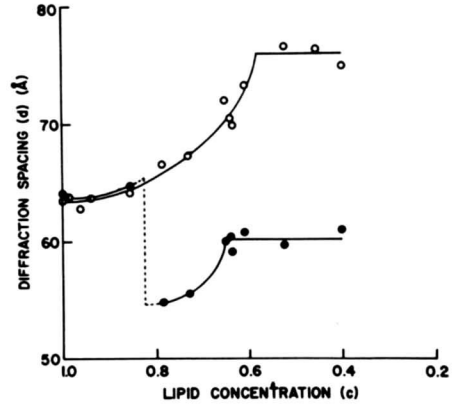

Fig. 4. Plot of X-ray diffraction spacing as a function of lipid concentration; ○, at 25°C; ●, at 47°C; ◐ represents overlapping points.

two endothermic peaks, separated by as much as 20°C, on heating (see, for example, mixture at c = 0.995 in Fig. 2*b*). On cooling, the same transitions are observed without significant supercooling (see Fig. 1, *d* and *e*). The temperature at which the two endothermic transitions occur decreases as the hydration level increases, and it appears that the temperature separation of the two transitions also decreases (Fig. 1, *c, d, f*). When the peak maxima are plotted as a function of lipid concentration (Fig. 2*b*), limiting values are reached for the two transitions in the range c = 0.85 to 0.80. The limiting values of the temperatures corresponding to the peaks of the two transitions occur at approximately 34 and 38°C. It is also interesting to note the absence of an ice–water melting transition at 0°C for the mixtures in the hydration range corresponding to c = 1.0–0.855.

X-ray diffraction

X-ray diffraction patterns were recorded at 25 and 47°C, corresponding, with the exception of low water contents, to temperatures below (25°C) and above (47°C) the thermal transitions observed by the microscope and DSC experiments. In all cases, in the low-angle region of the diffraction pattern a series of diffraction lines in the ratio 1:0.5:0.33:0.25:. . . was observed corresponding to a one-dimensional lamellar organization. At 25°C, for $c \leqslant 0.95$ the wide-angle region of the diffraction pattern consisted of a single, fairly sharp diffraction line at 4.15 Å, suggesting an ordered configuration for the hydrocarbon region of the lamellar structure. For mixtures with c < 0.85, increasing the temperature to 47°C produced changes in the position of the low-angle diffraction lines, while still maintaining the ratio 1:0.5:0.33:0.25: . . . . The diffraction at wide angles confirms the removal of the 4.15 Å line and its replacement with a broad, diffuse line at 4.6 Å. An example of the diffraction patterns observed at temperatures below (25°C) and above (47°C) the phase transition is shown in Fig. 3.

A plot of the d_{100} reflection of the lamellar phases as a function of lipid concentration is given in Fig. 4. At 25°C, the lipid + water repeat distance, d, increases from 63.5 to 76.0 Å with increasing hydration in the range c = 1.0–0.58. At higher hydration levels, c < 0.58, the diffraction spacing is independent of the water content, demonstrating the existence of a two-phase system, the lamellar (lipid + water) "ordered" gel phase and excess water. At 47°C, in the concentration range c = 1.0–0.85, analogous swelling behavior is observed; d increases from 63.9 to 64.7 Å, and a diffraction line at 4.15 Å is present. At $c \simeq 0.85$, a decrease in d_{100} is observed and the 4.15 Å line is replaced by the diffuse line at 4.6 Å. In the concentration range 0.85 > c > 0.65, swelling of the lamellar liquid crystal phase is observed, d increasing from 54.8 to 60.2 Å. Again, no further increase in d_{100} occurs on increasing the hydration in the concentration range corresponding to c < 0.65, indicating the presence of a two-phase system, in this case the lamellar (lipid + water) liquid crystalline phase and excess water.

If the dimensions of the lipid component, d_l, remain constant in a region consisting of a single phase, d should be a linear function of (1−c)/c (10). For the gel phase at 25°C this is not so, and thus it is concluded that d_l must change on hydration. Assuming a ratio of the partial specific volumes of the two components $\bar{v}_w/\bar{v}_l$ of 1.11 and a molecular weight for sphingomyelin of 767, d_l and the surface area per lipid molecule, S, were calculated for each mixture. These data are listed in Table 2 and are plotted as a function of lipid concentration in Fig. 5. As the hydration increases (or c decreases), d_l decreases linearly from 63.5 Å at c = 1.0 to 42.8 Å at c = 0.609. Over this concentration range, S increases from 36.1 $Å^2$ to 53.6 $Å^2$ and the thickness of the water layer, d_w, also increases linearly from 0 to 30 Å.

Making the same assumption regarding the ratio of the partial specific volumes of the two components, similar

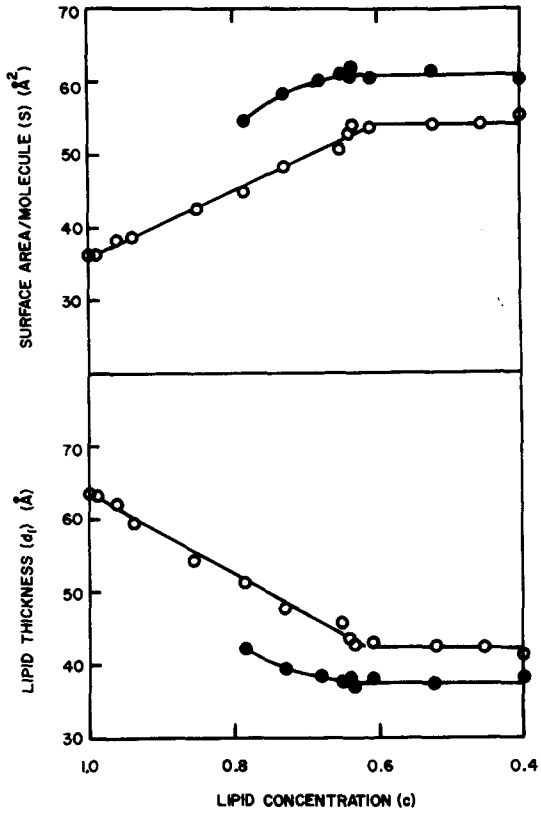

Fig. 5. Plot of lipid thickness and surface area per molecule as a function of lipid concentration. Parameters were calculated assuming a molecular weight for sphingomyelin of 767 and a ratio of the partial specific volumes of the two components ($\bar{v}_w/\bar{v}_l$) of 1.11; ○, at 25°C; ◐, at 47°C.

TABLE 2. Primary diffraction spacing (d), lipid thickness (d_l), and surface area per molecule (S) for sphingomyelin–water mixtures

Lipid concentration	25°C			47°C		
	d	d_l[a]	S[a]	d	d_l[a]	S[a]
	Å	Å	Å²	Å	Å	Å²
1.0	63.5	63.5	36.1	63.9	63.9	35.9
0.995	63.8	63.5	36.1	63.8	63.5	36.1
0.963	62.8	60.2	38.1			
0.939	63.7	59.4	38.6	63.7	59.4	38.6
0.855	64.2	54.1	42.4	64.7	54.5	42.1
0.786	66.6	51.1	44.9	54.8	42.1	54.5
0.729	67.3	47.7	48.1	55.5	39.3	58.4
0.650	72.0	45.1	50.9	60.0	37.6	61.1
0.640[b]	70.5	43.4	52.9	60.4	37.8	60.7
0.636[b]	69.9	42.7	53.7	59.1	37.0	62.0
0.609[b]	73.3	42.8	53.6	60.8	38.0	60.3
0.523[b,c]	76.6	42.4	54.1	59.7	37.4	61.4
0.455[c]	76.4	42.4	54.2			
0.400[b,c]	74.9	41.5	55.3	61.0	38.2	60.1

[a] All calculations were made assuming $\bar{v}_w/\bar{v}_l = 1.11$ and a molecular weight for sphingomyelin of 767.

[b] Calculations of d_l and S at 47°C were made assuming a limiting composition corresponding to c = 0.65.

[c] Calculations of d_l and S at 25°C were made assuming a limiting composition corresponding to c = 0.58.

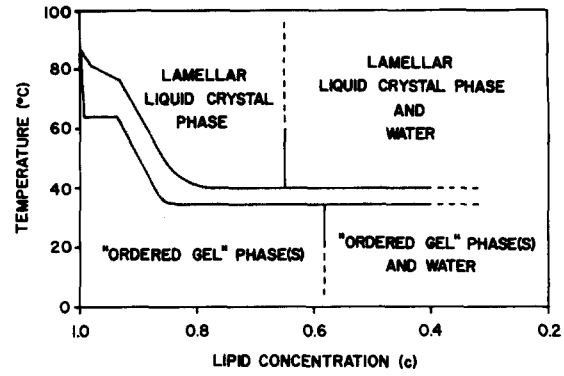

Fig. 6. Temperature–composition phase diagram of bovine brain sphingomyelin–water.

calculations of d_l and S for the swelling lamellar liquid crystal phase ($0.85 > c > 0.65$) at 47°C were made and are recorded in Table 2 and Fig. 5. The limiting value at c = 0.65 for the lipid thickness is approximately 38 Å, and the corresponding surface area is 60 Å².

DISCUSSION

A combination of the data obtained using the three techniques enables us to construct the condensed binary phase diagram shown in Fig. 6. Lamellar phases, in which water is intercalated between sheets of lipid molecules arranged in the classical bilayer fashion, are present over much of the phase diagram. An order–disorder transition separates the high temperature, liquid crystalline, lamellar phase from a more ordered lamellar phase at low temperatures. In the absence of water, sphingomyelin shows phase behavior similar to various lecithins. Up to a relatively high temperature, 87°C, a stable crystalline form is present, probably with the sphingomyelin molecules in the usual bilayer arrangement. At 87°C, a crystal–liquid crystal transition occurs, and the textural properties (neat phase texture) indicate the formation of a fairly mobile lamellar structure consisting of repeating units of apposed sphingomyelin bilayers. At 144°C, the formation of a viscous isotropic phase is observed, and the molecules are organized in such a way that one of the three-dimensional crystallographic cubic space groups is satisfied. Luzzati, Gulik-Krzywicki, and Tardieu (20) have described cubic phases formed by various lecithins in which finite-length rods of lipids are linked and interwoven in such a way that cubic symmetry results. It appears reasonable to expect a similar structural arrangement in the case of the structurally related sphingomyelin molecule. This phase transforms at 170°C to give the hexagonal type of structure (middle phase texture) in which "infinite" rods of lipid molecules, with the lipid head groups form-

ing the core of the rod, are packed in a regular two-dimensional hexagonal lattice. Since these various liquid crystal phases occur only at relatively high temperatures, no attempt was made to confirm their structure by X-ray diffraction methods.

The crystal–liquid crystal transition temperature(s) decreases as the water content increases and reaches a limiting value(s) at $c \simeq 0.80$. Above the line depicting the upper limit of the transition, at least up to 100°C, only the hydrated lamellar liquid crystal phase exists in which the hydrocarbon region can be considered to be disordered or liquidlike (α configuration [10]). Visual examination, light microscopy, and X-ray diffraction data confirm that this phase, like various lecithins (14, 20–22), cerebroside (23), and digalactosyl diglyceride (24), is of the limiting swelling type. Sphingomyelin at 47°C shows a limit in water uptake corresponding to 35% water by weight. At higher water contents the maximally swollen lamellar phase coexists with excess water. The limiting dimensions of this phase at 47°C, $d = 60.2$ Å, $d_l = 38$ Å, and $S = 60$ Å^2, differ significantly from the values given by Reiss-Husson (14) for maximally hydrated sphingomyelin at 40°C. On the basis of our data it seems probable that in the earlier study the transition to the liquid crystal phase was not complete at 40°C. This would account for the good agreement in the maximum repeat distance of the lamellar phase, 78 Å, with our value of 76 Å below the transition at 25°C. It seems unlikely that differences in the fatty acid composition could account for such large differences in the swelling characteristics. By comparing the swelling behavior of sphingomyelin at 47°C and egg yolk lecithin at 5°C (14), we see that at temperatures just above the phase transition both lipids incorporate approximately 35% water by weight and at maximum hydration have similar values for d, d_l, and S. Thus, it seems clear that the hydration or swelling characteristics are determined by the zwitterionic phosphatidylcholine polar head group common to both molecules.

Although the structure of sphingomyelin–water above the phase transition is well determined, the behavior of sphingomyelin below the transition offers at least two structural alternatives. At 25°C, sphingomyelin exists as a single lamellar lipid bilayer structure with water incorporated between the lipid bilayers in mixtures containing up to 42% water by weight. At higher hydration levels water exists as a separate phase. In the range $c = 1.0$–0.58, d increases from 63.5 to 76 Å as water is incorporated. However, the contribution of d_l to the overall lamellar repeat distance decreases on increasing hydration from 63.5 to 42.8 Å at $c = 0.609$, after which no change in d_l occurs (see Fig. 5). This decrease in lipid thickness is matched by an increase in the area occupied by each sphingomyelin molecule at the lipid–water interface, from 36.1 to 53.6 Å^2, over the same concentration range.

The presence of a single line at 4.15 Å in the wide-angle region would suggest an ordered or partially ordered phase with a regular packing of the hydrocarbon chains at 25°C. The β type of structure, in which the hydrocarbon chains pack with rotational disorder in a hexagonal lattice, the chain axes being normal to the surface of the lipid bilayer, may be excluded in this case on the basis of the calculations shown in Table 2 and Fig. 5. These data show that as the hydration increases, or c decreases, the lipid bilayer thickness decreases and surface area/molecule increases, whereas for the β structure both d_l and S should remain constant on increasing hydration. The second possibility is that the hydrocarbon chains pack according to a β' type of structure. In this case, although the hydrocarbon chains again pack in a pseudohexagonal lattice with rotational disorder, the axes of the chains may be tilted with respect to the plane of the lipid lamellae (21, 25). Furthermore, it has been shown recently for synthetic lecithins that the angle made by the hydrocarbon chain axis with the normal to the plane of the lamellae increases on increasing the hydration of the system (25). A comparison of the changes in d_l and S for sphingomyelin on increasing hydration with those for dipalmitoyl and distearoyl lecithins are in excellent agreement, the minor changes in slope and absolute values of the linear regions of the plot being attributable to hydrocarbon chain length differences and errors in the assumed ratios of the partial specific volumes of the two components.

Tardieu, Luzzati, and Reman (25) have suggested that only when two fatty acid chains of a phospholipid are identical, thus permitting a perfect molecular packing of the terminal methyl groups in the center of the lipid bilayer, can this β' structure be formed. For example, stearoyl-lauroyl lecithin does not form this phase (25). In the case of sphingomyelin, the hydration of this phase is significantly greater than for synthetic lecithin, and the value of 38° calculated for the maximum angle of tilt may pose problems in terms of molecular packing. In a systematic study of lipid–water systems at low temperatures, Tardieu (26) and Tardieu et al. (25) have demonstrated the presence of a number of complex lamellar and non-lamellar (rectangular) phases. Although at this stage it is possible that the relatively simple fatty acid composition (predominantly $C_{18:0}$ and $C_{24:0}$) of sphingomyelin permits hydrocarbon chain packing of the β' type, it is conceivable that the behavior of d_l and S on increasing hydration may be accounted for by a more complex ordered lamellar structure. Further studies on the temperature dependence of (*a*) the breadth of the 4.15 Å line, (*b*) the structural parameters d_l and S, and (*c*) one-dimensional Fourier syntheses across the lipid bilayer may result in an unequivocal structural description of this phase.

The surface area per molecule occupied by anhydrous sphingomyelin at 25°C, calculated from the X-ray diffrac-

tion and chemical data, is 36.1 A^2 (see Table 2). Assuming that the wide-angle diffraction line at 4.15 Å represents the interplanar separation of hexagonally packed hydrocarbon chains, a minimum value for the surface area occupied by two chains, or one molecule, is $2 \times 4.15^2 \times \sqrt{1/3} = 39.8$ Å^2. The former value may be low due to an error in the assumed value for $\bar{v}_l$, since a variation in $\bar{v}_l$ between 0.9 and 1.1 ml/g results in surface areas varying between 36.1 and 44.1 Å^2. A value of 44 Å^2 for the surface area of sphingomyelin at the air–water interface has been derived by monolayer studies (12, 13), whereas chemical separation of the two major chemical species of sphingomyelin results in a surface area of 40 Å^2 for a stearic acid-rich fraction and 56 Å^2 for a nervonic acid-rich fraction (27). Further monolayer studies in our laboratory show that although the minimum surface area of sphingomyelin at 25°C is 44 Å^2, the surface rheology changes on lowering the temperature and a solid condensed film with a limiting area of 39.5 Å^2 is observed below 10°C. This value is in reasonable agreement with the surface areas calculated from the X-ray diffraction data.

The summary of the above information, which is presented in Fig. 6, indicates that the low temperature phase at $c < 0.65$, whether present as a single phase ($c > 0.58$) or two phases ($c < 0.58$), ejects interbilayer water as it goes through the transition to produce the lamellar liquid crystal phase of fixed composition and the ejected, or ejected plus original excess, water. The data presented in Table 2 show that at $c = 0.609$, for example, the water thickness ($d - d_l$) decreases from 30.5 Å in the ordered gel phase at 25°C to 22.8 Å in the lamellar liquid crystal phase at 47°C. The product of the area per lipid molecule and one-half the water thickness gives an indication of the volume of trapped interbilayer water per lipid molecule. This volume decreases from 817 Å^3/molecule at 25°C to 689 Å^3/molecule at 47°C, or from about 27 water molecules per lipid molecule at 25°C to about 23 at 47°C. This reduction in the amount of trapped water as sphingomyelin passes through the transition results either from changes in the interbilayer interactions due to the zwitterionic phosphorylcholine group having energy minima at different head-group separations across or between the lipid bilayers in the two cases or from a conformational change of the phosphorylcholine group, thus altering its capacity to bind water.

Of particular interest is the relatively high temperature at which the order–disorder transition takes place for this naturally occurring and, in terms of its fatty acid composition, structurally inhomogeneous, sphingomyelin. The stability of the crystalline form of anhydrous sphingomyelin is matched by its behavior in the presence of water, when the phase transition occurs in the range ~30–40°C. This is a much higher value than that shown by most naturally occurring phospholipids (and other lipids) in which chain unsaturation and heterogeneity dictate a low transition temperature (e.g., egg yolk lecithin, ~ −5°C). The upper limit of the transition (~ 44°C) at maximum hydration is similar to that observed with maximally hydrated dipalmitoyl lecithin (41.5°C). However, other sphingosine-containing lipids, such as cerebroside (transition temperature 70°C) (23), can have even higher transition temperatures.

The presence of two endothermic peaks in the DSC heating curves of hydrated sphingomyelin (see Fig. 1) may be related to the relatively simple fatty acid composition of sphingomyelin, in which 45% and 27% of the chains are derived from stearic ($C_{18:0}$) and nervonic ($C_{24:1}$) acids, respectively. If a sufficient amount of a single molecular species exists (e.g., sphingomyelin containing only the $C_{18:0}$ fatty acid), molecular aggregation or clustering of the different molecular species may occur which may then undergo independent melting phenomena. In this case one might expect to observe diffraction from the two independent species at temperatures below the two transitions, but no such evidence is obvious in the diffraction patterns recorded at 25°C.

Finally, it is interesting to note that for sphingomyelin, the relative amount of which increases with age in various animal tissues, the phase transition encompasses body temperature. If the sphingomyelin were uninfluenced by neighboring lipids and/or interaction with proteins, such regions in membranes or tissues would be inhomogeneous in the sense that a balance would exist between ordered and disordered structures. The effects of cholesterol and lecithin on this phase behavior, which may shed further light on the biological importance of sphingomyelin, particularly in terms of its role in aging, arterial tissue disease processes, and its possible lecithin-linked asymmetric distribution in erythrocyte membranes, will be the subject of subsequent reports.

The authors wish to acknowledge helpful discussions with Drs. V. Luzzati and A. Tardieu on the lipid structures that exist at low temperatures. Ms. Stefanie Siegel is thanked for typing the manuscript. This research was supported by U.S. Public Health Service grant AM 11453-06. One of us (L.S.A.) received support from the undergraduate college work-study program.

Manuscript received 26 July 1973; accepted 5 November 1973.

REFERENCES

1. Rouser, G., G. J. Nelson, S. Fleischer, and G. Simon. 1968. Lipid composition of animal cell membranes, organelles and organs. *In* Biological Membranes. D. Chapman, editor. Academic Press, London. 5–69.
2. de Gier, J., and L. L. M. van Deenen. 1961. Some lipid characteristics of red cell membranes of various animal species. *Biochim. Biophys. Acta.* **49:** 286–296.
3. Bretscher, M. S. 1972. Asymmetrical lipid bilayer structure for biological membranes. *Nature New Biol.* **236:** 11–12.

4. Bretscher, M. S. 1972. Phosphatidyl-ethanolamine: differential labelling in intact cells and cell ghosts of human erythrocytes by a membrane-impermeable reagent. *J. Mol. Biol.* **71:** 523–528.
5. Skipski, V. P. 1972. Lipid composition of lipoproteins in normal and diseased states. *In* Blood Lipids and Lipoproteins: Quantitation, Composition and Metabolism. G. J. Nelson, editor. Wiley-Interscience, Toronto. 471–583.
6. Böttcher, C. J. F., and C. M. van Gent. 1961. Changes in the composition of phospholipids and of phospholipid fatty acids associated with atherosclerosis in the human aortic wall. *J. Atheroscler. Res.* **1:** 36–46.
7. Smith, E. B. 1965. The influence of age and atherosclerosis on the chemistry of aortic intima. *J. Atheroscler. Res.* **5:** 224–240.
8. Rouser, G., and R. D. Solomon. 1969. Changes in phospholipid composition of human aorta with age. *Lipids.* **4:** 232–234.
9. Chapman, D., and D. F. H. Wallach. 1968. Recent physical studies of phospholipids and natural membranes. *In* Biological Membranes. D. Chapman, editor. Academic Press, London. 125–202.
10. Luzzati, V. 1968. X-ray diffraction studies of lipid–water systems. *In* Biological Membranes. D. Chapman, editor. Academic Press, London. 71–123.
11. Shipley, G. G. 1973. Recent X-ray diffraction studies of biological membranes and membrane components. *In* Biological Membranes. Vol. 2. D. Chapman and D. F. H. Wallach, editors. Academic Press, London. 1–89.
12. Shah, D. O., and J. H. Schulman. 1967. Interaction of calcium ions with lecithin and sphingomyelin monolayers. *Lipids.* **2:** 21–27.
13. Shah, D. O., and J. H. Schulman. 1967. The ionic structure of sphingomyelin monolayers. *Biochim. Biophys. Acta.* **135:** 184–187.
14. Reiss-Husson, F. 1967. Structure des phases liquide-cristallines de différents phospholipides, monoglycérides, sphingolipides, anhydres ou en présence d'eau. *J. Mol. Biol.* **25:** 363–382.
15. Oldfield, E., and D. Chapman. 1972. Molecular dynamics of cerebroside–cholesterol and sphingomyelin–cholesterol interactions: implications for myelin membrane structure. *FEBS Lett.* **21:** 303–306.
16. Long, R. A., F. E. Hruska, H. D. Gesser, and J. C. Hsia. 1971. Phase transitions in sphingomyelin thin films. A spin label study. *Biochem. Biophys. Res. Commun.* **45:** 167–173.
17. Elliott, A. 1965. The use of toroidal reflecting surfaces in X-ray diffraction cameras. *J. Sci. Instrum.* **42:** 312–316.
18. Rosevear, F. B. 1954. The microscopy of the liquid crystalline neat and middle phases of soaps and synthetic detergents. *J. Amer. Oil Chem. Soc.* **31:** 628–639.
19. Small, D. M., M. C. Bourgès, and D. G. Dervichian. 1966. The biophysics of lipidic associations. I. The ternary systems: lecithin–bile salt–water. *Biochim. Biophys. Acta.* **125:** 563–580.
20. Luzzati, V., T. Gulik-Krzywicki, and A. Tardieu. 1968. Polymorphism of lecithins. *Nature.* **218:** 1031–1034.
21. Chapman, D., R. M. Williams, and B. D. Ladbrooke. 1967. Physical studies of phospholipids. VI. Thermotropic and lyotropic mesomorphism of some 1,2-diacyl-phosphatidylcholines (lecithins). *Chem. Phys. Lipids.* **1:** 445–475.
22. Small, D. M. 1967. Phase equilibria and structure of dry and hydrated egg lecithin. *J. Lipid Res.* **8:** 551–557.
23. Abrahamsson, S., I. Pascher, K. Larsson, and K.-A. Karlsson. 1972. Molecular arrangements in glycosphingolipids. *Chem. Phys. Lipids.* **8:** 152–179.
24. Shipley, G. G., J. P. Green, and B. W. Nichols. 1973. The phase behavior of monogalactosyl, digalactosyl and sulphoquinovosyl diglycerides. *Biochim. Biophys. Acta.* **311:** 531–544.
25. Tardieu, A., V. Luzzati, and F. C. Reman. 1973. Structure and polymorphism of the hydrocarbon chains of lipids: a study of lecithin–water phases. *J. Mol. Biol.* **75:** 711–733.
26. Tardieu, A. 1972. Etude cristallographique de systemes lipides–eau. Thesis, Doctorat d'Etat, Universite de Paris-Sud.
27. Raper, J. H., D. B. Gammack, and G. H. Sloane Stanley. 1966. A study of cerebral sphingomyelins in monomolecular films. *Biochem. J.* **98:** 21P.